LYMPHOID NEOPLASIA

Egress of CD19$^+$CD5$^+$ cells into peripheral blood following treatment with the Bruton tyrosine kinase inhibitor ibrutinib in mantle cell lymphoma patients

Betty Y. Chang,[1] Michelle Francesco,[1] Martin F. M. De Rooij,[2] Padmaja Magadala,[1] Susanne M. Steggerda,[1] Min Mei Huang,[1] Annemieke Kuil,[2] Sarah E. M. Herman,[3] Stella Chang,[1] Steven T. Pals,[2] Wyndham Wilson,[3] Adrian Wiestner,[3] Marcel Spaargaren,[2] Joseph J. Buggy,[1] and Laurence Elias[1]

[1]Research Department, Pharmacyclics, Inc., Sunnyvale, CA; [2]Pathology Department, Academic Medical Center, Amsterdam, The Netherlands; and [3]Hematology Branch, National Heart, Lung, and Blood Institute, National Institutes of Health, Bethesda, MD

Key Points

- MCL cells are mobilized into the peripheral blood of patients treated with the BTK inhibitor ibrutinib.
- Ibrutinib dose-dependently inhibits BCR- and chemokine-mediated adhesion and migration of MCL cells.

Ibrutinib (PCI-32765) is a highly potent oral Bruton tyrosine kinase (BTK) inhibitor in clinical development for treating B-cell lymphoproliferative diseases. Patients with chronic lymphocytic leukemia (CLL) often show marked, transient increases of circulating CLL cells following ibrutinib treatments, as seen with other inhibitors of the B-cell receptor (BCR) pathway. In a phase 1 study of ibrutinib, we noted similar effects in patients with mantle cell lymphoma (MCL). Here, we characterize the patterns and phenotypes of cells mobilized among patients with MCL and further investigate the mechanism of this effect. Peripheral blood CD19$^+$CD5$^+$ cells from MCL patients were found to have significant reduction in the expression of CXCR4, CD38, and Ki67 after 7 days of treatment. In addition, plasma chemokines such as CCL22, CCL4, and CXCL13 were reduced 40% to 60% after treatment. Mechanistically, ibrutinib inhibited BCR- and chemokine-mediated adhesion and chemotaxis of MCL cell lines and dose-dependently inhibited BCR, stromal cell, and CXCL12/CXCL13 stimulations of pBTK, pPLCγ2, pERK, or pAKT. Importantly, ibrutinib inhibited migration of MCL cells beneath stromal cells in coculture. We propose that BTK is essential for the homing of MCL cells into lymphoid tissues, and its inhibition results in an egress of malignant cells into peripheral blood. This trial was registered at www.clinicaltrials.gov as #NCT00114738. (*Blood*. 2013;122(14):2412-2424)

Introduction

Mantle cell lymphoma (MCL) is an aggressive type of B-cell malignancy, constituting 8% of non-Hodgkin lymphomas.[1-3] MCL is typically characterized by the t(11;14)(q13;q32) translocation, which drives cyclin D1 overexpression. Constitutive activation of the phosphatidylinositol 3-kinase/protein kinase B (PI3K/AKT) and nuclear factor κB pathways contribute to the pathogenesis of MCL.[1] The majority of MCL patients present with advanced disease at diagnosis, and more than 90% of patients have extranodal manifestations with circulating MCL cells, bone marrow, and gastrointestinal involvement. In general, MCL patients have a poor prognosis, with a median overall survival time of 30 to 43 months and fewer than 15% of them are long-term survivors.[2,3] This demonstrates a clear need for new therapeutics for the treatment of this disease.

The interaction of neoplastic B cells with stromal cells in the lymph node (LN) or bone marrow microenvironment plays a critical role in the survival, progression, and drug resistance of various B-cell malignancies,[4-7] including MCL.[6,8,9] Importantly, the homing and trafficking of B cells into the microenvironment is tightly controlled and regulated by the interaction of chemokine receptors and adhesion molecules.[10-15] The contact between MCL cells and mesenchymal stromal cells (MSCs) is established and maintained by chemokine receptors and adhesion molecules. Stromal cells in lymphoid tissues constitutively express chemokines such as CXCL12 and CXCL13, forming gradients that allow the homing of B lymphocytes from the periphery into tissue compartments. MCL cells express G protein–coupled chemokine receptors such as CXCR4 and CXCR5 that bind CXCL12 and CXCL13, respectively.[6] Adhesion is facilitated by binding of integrins such as VLA-4 on B cells to VCAM-1 on stromal cells and fibronectin in the extracellular matrix.[16] In addition to the chemokine receptor and integrin engagement, it has been shown that B-cell receptor (BCR) activation is involved in integrin (such as VLA-4) -mediated adhesion[7,14,16-18] and is thought to contribute to the growth and survival of most types of B-cell malignancies.[17,19-21] BCR signaling pathway phosphoproteins are represented abundantly in MCL cell lines,[1,22,23] and genomic lesions or constitutive activation of signaling proteins downstream of the BCR pathways such as SYK and PI3KA have been reported in MCL.[23-25]

Since BCR signaling is important for integrin-mediated adhesion, growth, and survival of B lymphocytes, Bruton tyrosine kinase

Submitted February 1, 2013; accepted August 2, 2013. Prepublished online as *Blood* First Edition paper, August 12, 2013; DOI 10.1182/blood-2013-02-482125.

M.F. and M.F.M.D.R. contributed equally to the manuscript.

The online version of this article contains a data supplement.

The publication costs of this article were defrayed in part by page charge payment. Therefore, and solely to indicate this fact, this article is hereby marked "advertisement" in accordance with 18 USC section 1734.

(BTK), a key component of the BCR pathway, is thus significant in B lymphocyte adhesion and survival.[7,14,16,18] More recently, it has been shown that BTK plays a role in chemokine (such as CXCL12) -controlled B-cell chemotaxis and homing.[14] The BTK inhibitor ibrutinib (PCI-32765) is an irreversible covalent inhibitor with a 50% inhibitory concentration of 0.5 nM against BTK in biochemical assays, has been found to have broad antitumor activity in B-cell malignancies including MCL,[26,27] and is currently being evaluated in phase 3 clinical studies. In the initial phase 1 study, we noted that many MCL patients had rapid increases of $CD5^+$ B lymphocytes in the peripheral blood (PB) following ibrutinib treatment. This often occurred concomitantly with rapid reductions of lymphadenopathy, suggesting an egress of malignant cells from tissues into PB. The schedule of drug administration for most patients in the phase 1 study was in cycles of daily administration for 28 days, followed by 7 days without drug administration. We observed that the lymphoid flux was rapidly reversed during the 7-days-off portion of the treatment, with prompt reappearance at the beginning of the next cycle, resulting in a sawtooth pattern in PB. These patterns, along with immunophenotypic characterization of the cells involved, are presented here. We further investigated the mechanism of this effect by using MCL cell lines and primary cells and also in an MCL–stromal coculture system. We demonstrated that ibrutinib suppressed BCR- and CXCL12-/CXCL13-mediated adhesion and chemotaxis, suppressed migration of cells beneath the stromal cells (pseudo-emperipoiesis), and inhibited the phosphorylation of BTK, PLCγ, and ERK in MCL cells. These observations effectively highlight the importance of BTK catalytic activity in the homing of MCL cells into lymphoid tissues and provide insight into the relevant mechanisms.

Materials and methods

Refer to supplemental Methods for details (available on the *Blood* Web site).

Primary human MCL specimens from drug-treated patients

Blood was drawn from MCL patients enrolled in PCYC-04753[26] or PCYC-1104[27] (before April 1, 2012) in accordance with International Conference on Harmonisation Good Clinical Practice guidelines and principles of the Declaration of Helsinki, with informed consent from each patient and in compliance with the protocols approved by the relevant institutional review board. The blood samples were drawn into sodium heparin cell preparation tubes (BD) and shipped overnight to Pharmacyclics, Inc., within 24 hours. In a laminar flow hood, the peripheral blood mononuclear cells (PBMCs) were collected, washed with phosphate-buffered saline (PBS), and frozen in 90% fetal bovine serum and 10% dimethylsulfoxide in liquid nitrogen until use.

Cell lines and primary material for ex vivo studies

Adhesion studies were performed with PBMCs from MCL patients of the Academic Medical Center (Amsterdam, The Netherlands). For ex vivo CXCR4 and CD38 staining studies, PB and LN biopsies were collected from treatment-naive MCL patients enrolled in National Cancer Institute Study 05-C-0170 (www.clinicaltrials.gov #NCT00114738) with approval from the National Institutes of Health Institutional Review Board and informed consent. Matched PB and LN samples were obtained on the same day and were processed and analyzed in parallel.

MCL phenotyping

PBMCs were washed, pelleted, and resuspended in PBS and 2% fetal bovine serum containing phenotyping surface antibodies. All staining cocktails were run in duplicate tubes. Cells were stained for 30 minutes, washed, pelleted, and fixed in PBS and 1.6% paraformaldehyde. Cells to be analyzed for proliferation with Ki67 were permeabilized with 70% ethanol at −20°C overnight, rehydrated with PBS, and stained with Ki67 antibody.

Flow cytometry

BD FACS (fluorescence-activated cell sorter) Canto II was used for all flow cytometry collections. Phosphoflow assays were stained and performed as described.[28] At least 10 000 $CD19^+$ cells were collected from each staining sample. The data were analyzed and quantified by using FlowJo v7.6, and the geometric mean was derived and presented for the mean fluorescence intensities (MFIs) of histograms for the specifically stained cell populations.

Coculture assays

Cocultures of M2-10B4 stromal cells and the MCL cell line Mino were established according to Burger et al.[10] Mino cells were treated with vehicle, pertussis toxin, or ibrutinib for 1 hour at 37°C and then added to confluent monolayers of stromal cells. The cocultures were incubated at 37°C for 5 hours to overnight to allow migration of Mino cells beneath the stromal cell layer, after which they were washed extensively to remove unmigrated cells. For cocultures using live-cell tracer dyes, M2-10B4 and Mino cells were first loaded with CellTracker Green 5-chloromethylfluorescein diacetate (CMFDA) and CellTracker Orange 5-(and-6)-(((4-chloromethyl) benzoyl)amino)tetramethylrhodamine (CMTMR), respectively. For microscopy, cells were fixed with paraformaldehyde and mounted on slides with 4,6 diamidino-2-phenylindole mounting medium (Vectashield). For quantification of migration of Mino cells in cocultures by flow cytometry, cells were trypsinized and stained with APC-Cy7–labeled anti-CD19 antibody. Cells were counted by using CountBright absolute counting beads (Life Technologies).

Actin polymerization in Mino cells

Mino cells were adhered to coverslips in serum-free media for 30 minutes at 37°C and treated with dimethylsulfoxide, pertussis toxin, or ibrutinib for 1 hour. Cells were fixed with paraformaldehyde, permeabilized with Triton X-100, and stained with Alexa Fluor 594–labeled phalloidin (Molecular Probes). Coverslips were mounted on glass slides by using Vectashield mounting medium containing 4,6 diamidino-2-phenylindole. Microscopy was performed on a Zeiss Axioplan 2 microscope using a 63×/1.40 oil immersion Plan-Apochromat objective, and images were acquired with a Zeiss AxioCam MRm charge coupled device camera and AxioVision v.4.8 software. For densitometry, at least 30 cells were imaged for each condition.

Adhesion and migration assays

Cell adhesion[7,14] and migration assays were performed as described.[14,29]

Immunoblotting

Western blots were performed as previously described.[7,29]

Statistical analysis

Analyses were performed by using GraphPad Prism 4.0. Statistically significant differences were determined by using either analysis of variance with Bonferroni's post hoc comparison, or unpaired two-tailed Student *t* test was used to determine the significance of differences between two means. The one-sample *t* test was used to determine the significance of differences between means and normalized values (100%).

Results

Transient increase in absolute lymphocyte count following ibrutinib administration to MCL patients

In a phase 1 study that enrolled patients with various non-Hodgkin lymphomas, MCL patients were treated with ibrutinib in 35-day

cycles during which the drug was administered once a day for 28 days with a 7-day drug holiday between cycles.[26] Under these conditions, a cyclical pattern of increasing and decreasing absolute-lymphocyte count (ALC) was observed. This was demonstrated by an increase in ALC following the first few weeks of treatment followed by a return to baseline after the 7-day drug holiday (Figure 1A). This cyclic ALC pattern continued for the duration of the treatment (data not shown). During the course of ibrutinib treatments, tumor volumes (quantified by sum of perpendicular diameters measurements from scans) decreased by 75% on average (Figure 1A) during 2 to 6 treatment cycles. Thus, during the first 6 cycles of treatment, the cyclic changes of PB ALC occurred concomitantly with nodal responses in these patients. The increase in ALC was observed in a subsequent (phase 2) study in which MCL patients were treated with a fixed continuous daily dose of 560 mg without interruption. In this trial, the ALC increased by 100% to 200% following the first 2 to 4 weeks of treatment, followed by notable gradual reductions in ALC commencing by the eighth week of treatment and continuing over the following months (Figure 1B).

Elevated ALC is due to an increase of light chain–restricted $CD19^+CD5^+$ cells

In order to define the population of lymphocytes increased by ibrutinib, the PBMCs of patients isolated before (day 1 [D1]) and after 1 week of treatment (day 8 [D8]) were stained with CD3, CD19, and CD5 and analyzed by flow cytometry. The increased lymphocytes were characterized as $CD3^-CD19^+CD5^+$; both the absolute count and the percentage of $CD19^+CD5^+$ cells in the lymphocyte population were significantly increased after 1 week of ibrutinib treatment ($P < .05$), whereas the absolute count and the percentage of $CD19^+CD5^-$ cells was not (Figure 1C). An illustrative patient is shown in Figure 1D, in whom the $CD19^+CD3^-$ and $CD19^+CD5^+$ populations before drug treatments were 9.29% and 84.4%, respectively, and they increased to 63% and 98.8% after 1 week of treatment. The $CD19^+CD3^-CD5^+$ cells were light chain–restricted (data not shown), likely reflecting increased circulating MCL cells in the periphery following 1 week of drug treatment. In some cases, the mobilized cells made up a distinct subset of $CD45^{dim}$ small cells, which is also consistent with MCL (data not shown).

To confirm that full inhibition of the target BTK was achieved in these patients, occupancy of the BTK active site by ibrutinib was assessed in PBMCs from MCL patients by using a competitive binding fluorescent probe assay.[30] On average, more than 90% target occupancy was observed in patients following 1 week of treatment (Figure 1E-F).

The peripheral $CD19^+CD5^+$ population has decreased Ki67, pERK, and surface CD38 and CXCR4 expression following drug treatment

Peripheral $CD19^+CD5^+$ cells were analyzed for markers commonly associated with cell proliferation/activation states such as CD38,[31,32] Ki67,[33] and pERK. $CD38^+$ surface expression was higher in the $CD19^+CD5^+$ cells than in the normal $CD19^+CD5^-$ cells prior to drug treatment and became even higher in some patients immediately after treatment (Figure 2A), likely because of the higher CD38 expression in tissues (Figure 2D), but it decreased significantly following 1 week of treatment ($P < .05$) (Figure 2B) and decreased even further with longer treatment, while the CD38 expression in the normal B cells did not change (Figure 2A). In vitro ibrutinib treatment did not affect CD38 expression in MCL cells (supplemental Figure 1). Furthermore, Ki67 expression, commonly used as a marker of proliferation, was significantly reduced after treatment ($P < .01$) (Figure 2B; supplemental Figure 7). pERK expression was generally higher in the $CD20^+CD5^+$ cells of MCL patients compared with healthy volunteers and was significantly reduced by ibrutinib treatment (Figure 2B, lower panel; $P < .05$).

Since the chemokine receptor CXCR4 is important for B-cell homing to lymphoid tissues,[34,35] we determined the surface CXCR4 expression in the MCL cells and found that CXCR4 was significantly reduced ($P < .05$) in the $CD19^+CD5^+$ population following 1 week of treatment (Figure 2C). We then analyzed CXCR4 expression on patient-matched LN- and PB-resident MCL cells from 3 untreated patients and found that CXCR4 expression was lower in MCL cells isolated from LNs compared with PB in all 3 patients examined (Figure 2D), similar in trend to those noted in chronic lymphocytic leukemia (CLL) patients in whom CXCR4 surface expression is lower in LN compared with PB[36,37] because of receptor endocytosis from high tissue concentrations of CXCL12.[4,10,36,38] Therefore, the newly circulating $CXCR4^{lo}$ MCL cell population is consistent with the mobilized cells originating from tissues such as LNs. This interpretation is further supported by the notable reduction in lymphadenopathy observed during the same period (Figure 1A). Importantly, ibrutinib treatment in vitro did not have a direct effect on CXCR4 surface expression in primary MCL cells at concentrations of 1 to 1000 nM (supplemental Figure 1).

We also examined changes to plasma chemokines in the treated patients and found that chemokines important in B-cell trafficking/homing (CXCL13) and T-cell/accessory-cell attractions (CCL22, CCL4, CCL17)[6,39,40] were reduced on average by more than 50% following 1 week of treatment. By the end of the first cycle of treatment, in addition to the decrease of CCL4 and CCL22, cytokines important for MCL proliferation—interleukin 10 (IL-10) and tumor necrosis factor α (TNF-α)[41,42]—were also reduced by 50% (Figure 2E).

Ibrutinib inhibits pseudo-emperipoiesis in MCL–stromal coculture

The transient increase of ALC in MCL patients treated with ibrutinib may be due to a disruption in cellular adhesion and migration within the LN or tissue compartment. To investigate this, we established the in vitro effect of ibrutinib on the pseudo-emperipoiesis of MCL in stromal cell cocultures. Primary MCL cells or the Mino cell line were grown in coculture with M2-10B4 murine bone marrow stromal cells. We found that primary MCL cells or Mino cells both adhered to and migrated beneath the M2-10B4 cells. Significant inhibition of pseudo-emperipoiesis by ibrutinib was observed, as demonstrated by light microscopy (Figure 3A-B), and the number of Mino cells or primary MCL cells remaining in the coculture were quantified by flow cytometry of $hCD19^+$ cells harvested by gentle washing following 4 hours of coculture (Figure 3D-E, left panels). Ibrutinib dose-dependently inhibited migration of Mino cells beneath the stromal cells, and the inhibition was significant at 100 nM ($P < .01$) and 1000 nM ($P < .001$). Pertussin toxin, a well-studied G protein coupled receptor inhibitor used as a positive control for inhibition of Mino cell migration significantly inhibited migration at 200 ng/mL ($P < .001$). In addition, CXCL12, an important chemokine for B-cell homing produced by stromal cells, increased cortical actin of Mino cells, as assessed by phalloidin fluorescence microscopy, and this response was also dose-dependently and significantly inhibited by ibrutinib treatments at 10 and 100 nM ($P < .001$) (Figure 3C-D, right panel). Ibrutinib also suppressed actin polymerization of primary MCL in coculture at 100 nM ($P < .001$) (Figure 3E, right panel).

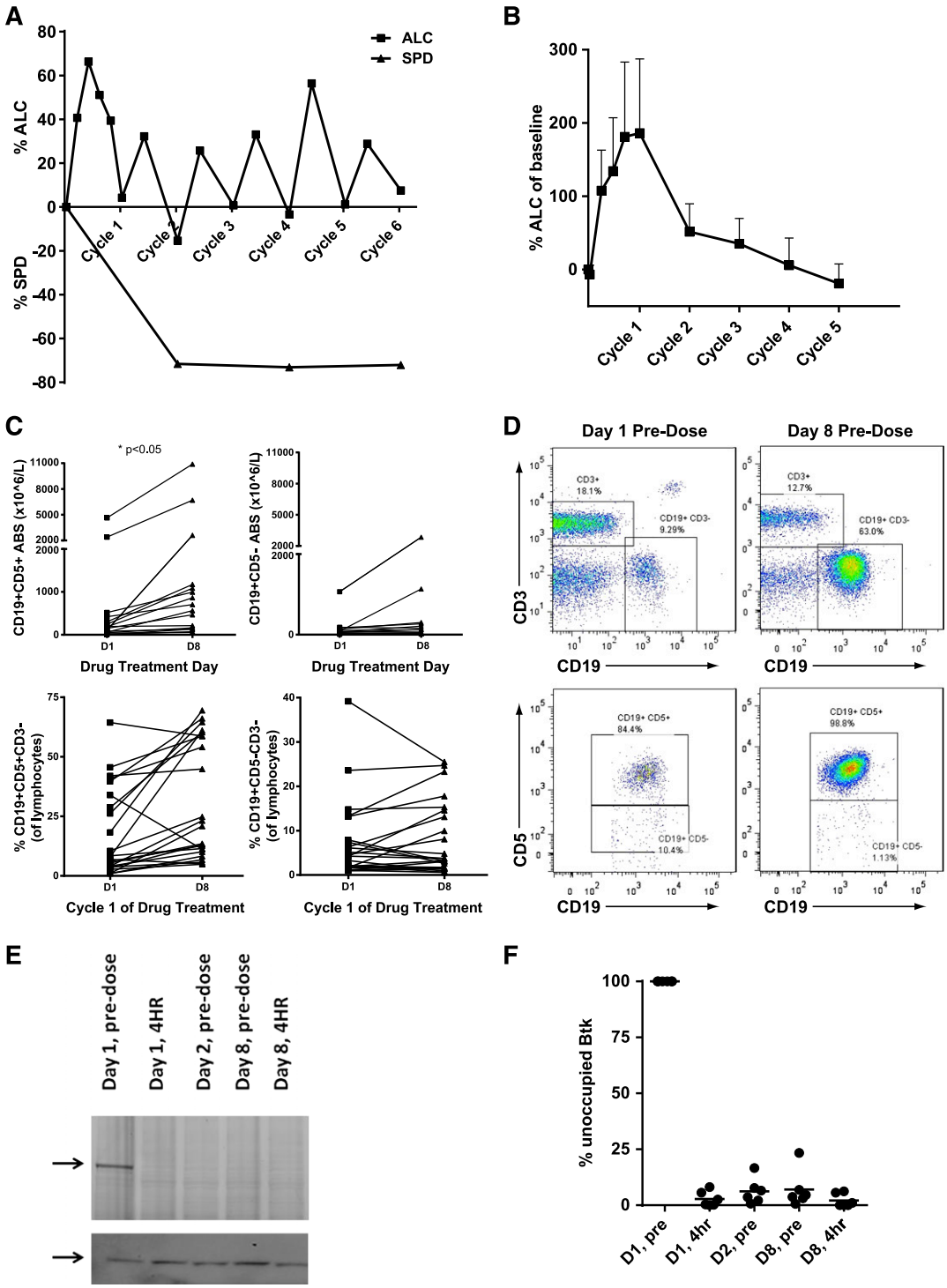

Figure 1. Transient mobilization of lymphocytes in MCL patients treated with ibrutinib. The mean percentage change of ALC (over baseline) is graphed against treatment time. (A) Ibrutinib treatment was in 35-day cycles of 28 days on and 7 days off. Mean percentage ALC change and percentage of the sum of perpendicular diameters (SPD) change are plotted to treatment cycles (n = 9). (B) Ibrutinib treatment was continuous with no gap in treatment. Mean percentage ALC change compared with baseline (plotted as mean + standard error [SE]; n = 17) is plotted against treatment time. Time points plotted are D0 (day zero), D1, D8, D15, D22, and end of cycles 1, 2, 3, 4, and 5. (C) The absolute count (ABS) and percentage of $CD19^+CD5^+$ vs $CD19^+CD5^-$ cells following 1 week of ibrutinib treatment. Note the statistically significant change in the absolute count of $CD19^+CD5^+$ cells of MCL patients following treatment. $^*P < .05$ (paired *t* test; n = 16). (D) Flow plot of gated lymphocytes of PBMC samples from a representative MCL patient before and after ibrutinib treatment (560 mg per day) for 7 days. PBMCs were stained with CD3, CD19, and CD5. Note increase of $CD19^+CD3^-$ and $CD19^+CD5^+$ population after 7 days of drug treatment. (E) Fluorescent probe occupancy assay of BTK in PBMCs isolated from a representative MCL patient before treatment (predose), and after 4 hours, 24 hours after first dose, before treatment on the eighth day (Day 8, predose), and 4 hours after the eighth day dose (Day 8, 4HR). The arrows point to the 75 kDa BTK band on a scanned fluorescent gel (top) and a western blot (bottom). (F) An average of >90% occupancy of BTK by drug is achieved in MCL patients who were administered ibrutinib in the first week, determined by fluorescent probe assays (n = 6).

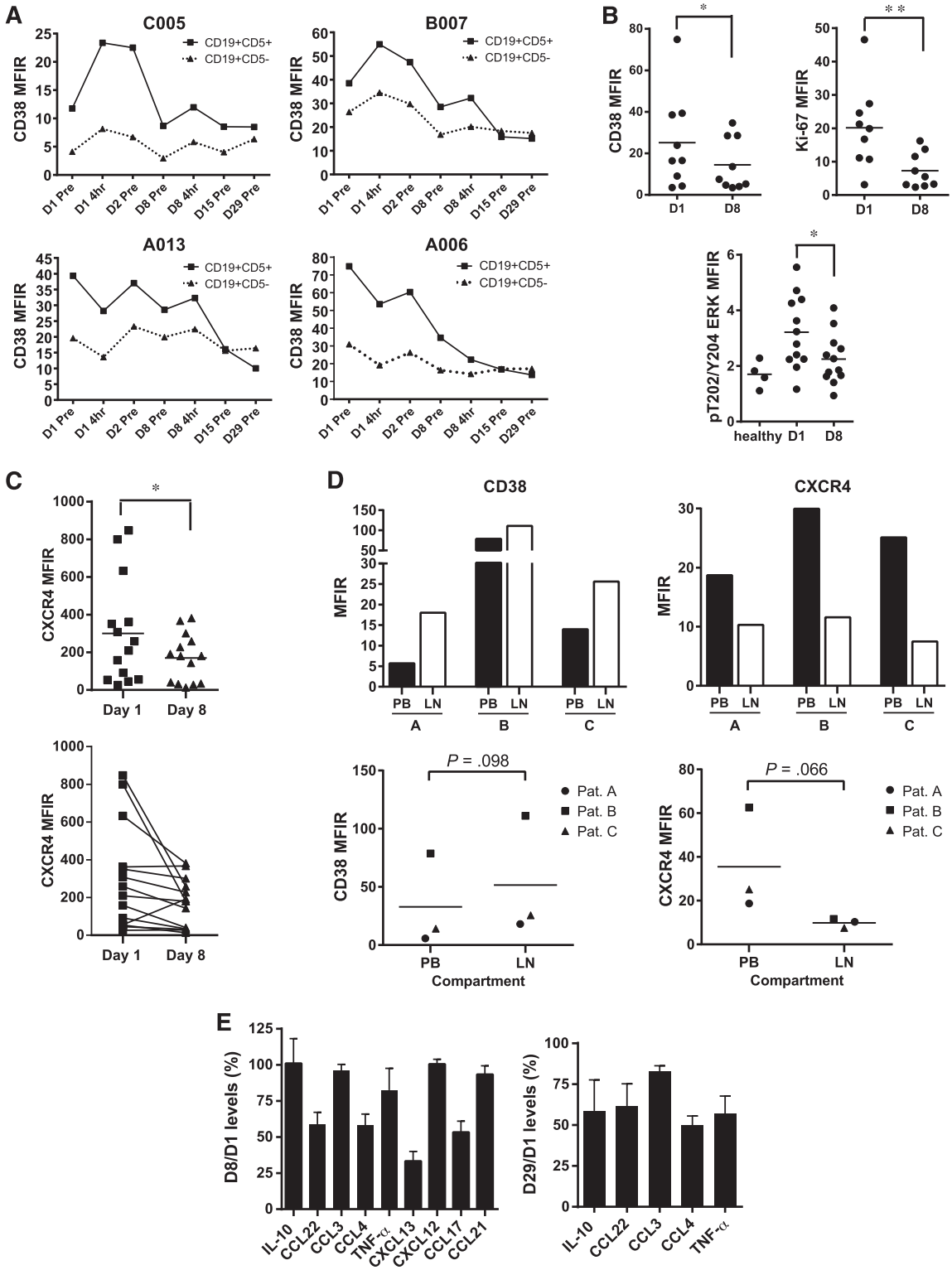

Figure 2. CD19$^+$CD5$^+$ cells have decreased CXCR4, CD38, and Ki67 expression following ibrutinib treatment. (A) Reduction of CD38 expression (mean fluorescence intensity ratio [MFIR]) in CD19$^+$CD5$^+$ cells but not CD19$^+$CD5$^-$ cells during 4 weeks of treatment in 4 patients treated with ibrutinib. (B) Surface CD38 expression (left panel; *$P < .05$) and intracellular Ki67 (right panel; **$P < .01$) is significantly reduced following 1 week of treatment. MFIR of intracellular phospho-ERK (pT202/Y204/ERK1/2) of CD20$^+$CD5$^+$ cells from healthy participants or MCL patients treated with ibrutinib before treatment (day 1 [D1]) and after 1 week of treatment (D8) (lower panel; *$P < .05$). (C) Significant reduction of surface CXCR4 expression (MFIR) in CD19$^+$CD5$^+$ cells following 1 week of ibrutinib treatment (n = 14; *$P < .05$). The line between the dot plots shows the mean. (D) CXCR4 and CD38 expression from LN biopsies and PBMCs (PB) of three MCL patients (patients A, B, and C) not treated with drug. (E) Plasma chemokine and cytokine concentrations on day 8 (D8; left) or day 29 (D29; right) of ibrutinib-treated MCL patients compared with pretreatment times 100% (n = 9).

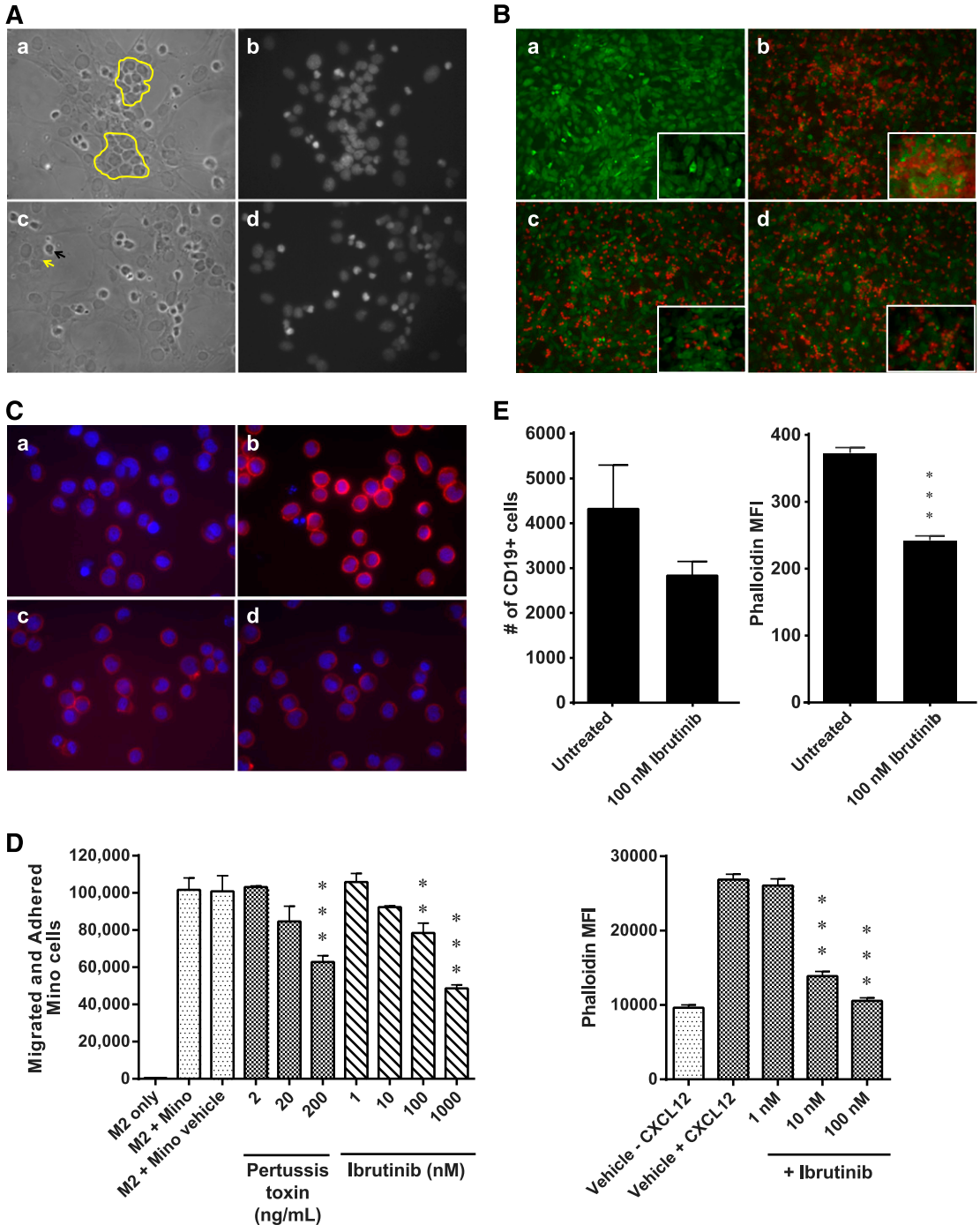

Figure 3. Ibrutinib inhibits migration of MCL cells beneath stromal cells (pseudo-emperipoiesis) and the formation of CXCL12-stimulated cortical actin. (A) Phase contrast (left panel) and 4,6 diamidino-2-phenylindole (DAPI) staining (right panel) of Mino and BM stromal cell M2-10B4 coculture 24 hours after Mino cells were pretreated with vehicle (dimethylsulfoxide [DMSO]) (panels a and b) or ibrutinib (1000 nM) (panels c and d). Highlighted yellow outlines show typical cobblestone appearance of migrated Mino cells beneath stromal cells. Black arrow points to a cell that is adhered on top of stromal cells but not migrated underneath. Yellow arrow points between two migrated Mino cells. (B) Mino cell and stromal cell coculture of Mino cells loaded with 5-(and-6)-(((4-chloromethyl)benzoyl)amino)tetramethylrhodamine (red), and M2 cells loaded with 5-chloromethylfluorescein diacetate (green). (A) Stromal cells alone and (B) in coculture with Mino cells. (C) Mino cells pretreated with G protein coupled receptor inhibitor pertussis toxin at 200 ng/mL or (D) ibrutinib at 1000 nM. (C) Mino cells were stimulated with CXCL12 at 100 ng/mL and stained with rhodamine-phalloidin to determine actin polymerization and were counterstained with DAPI to identify nuclei of cells. Phalloidin staining of Mino cells (A) before and (B) after CXCL12 stimulation and after treatment with (C) pertussis toxin at 200 ng/mL or (D) ibrutinib at 100 nM. Magnification, ×200. (D) Mino cells were pretreated with ibrutinib, pertussis toxin, or vehicle for 30 minutes and then placed on a stromal cell–populated plate. After 4 hours, coculture was washed several times and migrated, and adhered Mino cells were counted in a flow cytometer with calibrated beads after staining with hCD19. Both pertussis toxin and ibrutinib dose-dependently inhibited migration and adhesion of Mino cells (left panel). Mino cells stimulated with CXCL12 and treated with vehicle or drug were stained with phalloidin, and its intensity was determined by using flow cytometry (right panel). (E) Ibrutinib (100 nM) inhibited pseudo-emperipoiesis of primary MCL ($hCD19^+$ cells) in coculture with M2-10B4 stromal cells (left panel). Actin polymerization as assessed by phalloidin staining was significantly reduced by ibrutinib treatment in primary MCL cells. $^{**}P < .01$; $^{***}P < .001$. One-way analysis of variance (ANOVA) compared with vehicle control.

Ibrutinib inhibits BTK activity in MCL/stromal cell coculture and suppresses stromal cell–induced chemokine and cytokine secretion

To further understand the drug effect on MCL cells in coculture with stromal cells, Mino cells were treated with drug and cocultured with M2-10B4 or stimulated with anti-immunoglobulin M (IgM). Ibrutinib dose-dependently inhibited pBTK, pPLCγ2, pAKT, and pERK in Mino cells in coculture with M2-10B4 cells and in Mino cells with BCR stimulation (Figure 4A). Chemokine and cytokine concentrations of conditioned media were determined from ibrutinib-treated Mino cells alone or stimulated with anti-IgM or in coculture (Figure 4B). Mino cells increased chemokine and cytokine secretions following BCR stimulation or coculture with M2 cells. Similar results were observed with the Jeko cell line (supplemental Figure 2). Ibrutinib dose-dependently and potently suppressed production of human IL-10, CCL22, CCL3, CCL4, TNF-α, and CCL17 following BCR activation or in coculture, whereas the murine stromal cells alone did not produce human chemokines or cytokines (Figure 4B). Similarly, ibrutinib suppressed the production of IL-10, CCL22, CCL3, CCL4, and TNF-α of Jeko1 cells in coculture with M2-10B4 (supplemental Figure 2) or human stromal cell line HS-5 (data not shown). Interestingly, these chemokines/cytokines were also reduced in ibrutinib-treated patients, but the degree of reduction in plasma CCL3 was far less than that in vitro (Figure 2E).

Ibrutinib inhibits BCR- and chemokine-mediated adhesion and migration in vitro

We measured the direct effect of ibrutinib on adhesion and migration of the MCL cell lines Jeko1, HBL2, Mino, and JVM-1. First, the effect of ibrutinib on BTK signaling was determined. As expected, ibrutinib inhibited phosphorylation of BTK and downstream signaling proteins PLCγ2, MAP kinases ERK, JNK, and AKT following stimulation by anti-IgM and chemokines CXCL12 and CXCL13 (Figures 5A-B and 6A; supplemental Figures 5 and 6). Cell surface expression of CXCR4, CXCR5, CCR7, surface IgM, and α4β1 integrin was confirmed by flow cytometry (supplemental Figure 3), and subsequent in vitro adhesion and chemotaxis assays were performed with the drug. Ibrutinib significantly inhibited anti-IgM–stimulated adhesion of Jeko1 and HBL1 cells onto fibronectin or VCAM-1 at 100 nM (a clinically relevant concentration of ibrutinib) with more than 50% to 70% inhibition. The inhibition of adhesion by ibrutinib was also dose-dependent (supplemental Figure 4). Similarly, the adhesion of both Mino and Jeko1 cells to VCAM-1 or fibronectin was inhibited by ibrutinib at 100 nM following CXCL12 or CXCL13 activation. The extent of inhibition was greater in Mino cells (50% to 70%) than in Jeko1 cells (20% to 30%) (Figure 6B-C). We found that, in addition to changes in adhesion, ibrutinib dose-dependently inhibited CXCL12-induced migration of Mino, Jeko1, and JVM-1 cells, with Mino and Jeko1 cells being more sensitive to drug than JVM-1 cells (Figure 6D). Ibrutinib also significantly inhibited CXCL13-stimulated migration of Mino cells dose-dependently from 1 nM to 1 μM (Figure 6D).

Next, we examined the effect of ibrutinib on signaling and adhesion in primary MCL cells. In primary MCL, pY223BTK was increased compared with that in normal B lymphocytes, consistent with elevated BCR signaling in malignant B cells. Ibrutinib inhibited pBTK in both primary MCL and normal B cells on Y223, the autophosphorylation site of BTK, and Y551 (phosphorylated by Src family kinases) and reduced pPLCγ2 on Y759 and Y1217 (Figure 7A) at concentrations of 10 nM and above. These results demonstrate that ibrutinib directly inhibits BTK activity in MCL primary cells. Importantly, ibrutinib also inhibited CXCL12- or CXCL13-activated adhesion to VCAM-1 as well as BCR-stimulated adhesion to fibronectin at 100 nM in primary MCL cells. The degree of inhibition in these primary cells was about 10% to 20%, and the magnitude was less impressive compared with that in the MCL cell lines but the inhibition was statistically significant (Figure 7B).

These studies collectively demonstrate that ibrutinib inhibits BCR-, CXCL12-, and CXCL13-activated adhesion and migration in MCL cell lines as well as in primary MCL cells, which is associated with the BTK inhibition in these cells.

Discussion

Dramatic early increases of PB lymphocytes occur consistently among CLL patients treated with small-molecule antagonists of the BCR signaling pathway (Syk, PI3Kδ, and BTK inhibitors).[26,43,44] Here we report and characterize similar early transient elevations of lymphocytes among MCL patients treated with the irreversible BTK inhibitor ibrutinib. The increase in ALC commenced as early as the first week, was maximal after 2 to 3 weeks of treatment, and then gradually subsided over several cycles of treatment. As with CLL patients,[26] MCL patients dosed on a 28-days-on and 7-days-off schedule exhibited decreases of ALC following the 7-day-off period at the end of each cycle, and subsequent increases of ALC were observed periodically at the beginning of each subsequent cycle. Despite these increases in circulating cells, lymphatic masses were noted to decrease concomitantly, consistent with cellular mobilization from tissues as opposed to disease progression.

We found that the newly appearing cells were light chain–restricted $CD19^+CD5^+$ cells, consistent with their identification as MCL cells. The identity of these cells as lymphomatous is not surprising since circulating PB tumor cells are often detectable among patients with MCL. Increase of circulating MCL cells following treatment has not been previously reported and, moreover, it was highly specific, not involving $CD19^+CD3^-CD5^-$ cells. Importantly, the $CD19^+CD5^+$ cells exhibited significantly lower CD38, Ki67, and pERK (downstream to BTK[30]) markers of cell activity. In addition, surface expression of CXCR4 was decreased. Consistent with studies on CLL cells, we found that MCL cells have lower expression of CXCR4 in LNs compared with PB. The shift in CXCR4 expression may thus largely reflect release from LNs or other tissues rather than a direct reduction of CXCR4 expression on circulating MCL cells because in vitro studies showed no effect of drug on surface CXCR4 on primary MCL cells (supplemental Figure 1). $CXCR4^{hi}$ CLL cells have been shown to be able to reenter tissues and LNs, whereas $CXCR4^{lo}$ CLL cells likely have just exited tissues and can no longer reenter lymphoid organs.[17,36,37] Thus, the increase in MCL cells is likely to be derived from newly egressed MCLs from tissues and LNs. However, if these egressed MCLs just exited from tissues, why are they $CD38^{lo}$ since LN cells are $CD38^{hi}$? A closer look at CD38 expression in the first few days following drug treatment showed an initial increase of CD38 followed by a gradual decrease of expression over time (Figure 2A). In CLL, CD38 expression serves as a real-time indicator for cell proliferation and activity,[31] and we speculate this may be true for MCL. The newly circulating MCL cells, having been exposed to target-saturating concentrations of ibrutinib, are likely to be less proliferative, as indicated by reduced Ki67, a prognostic marker for outcome of advanced MCL survival[3,33] and pERK. Malignant CLL cells have been shown

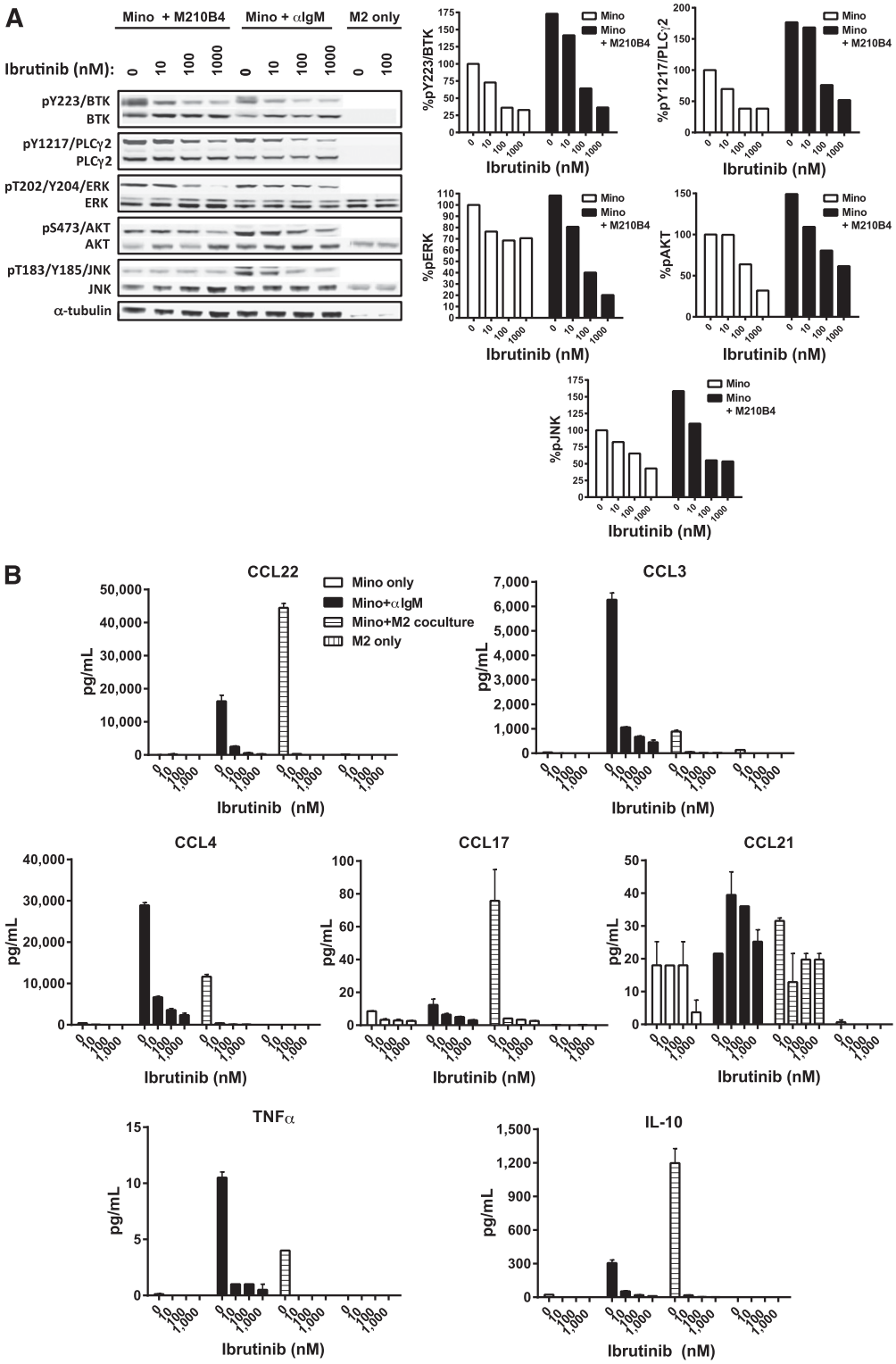

Figure 4. Ibrutinib suppresses BCR- and coculture-stimulated signaling and cytokine and chemokine production of MCL cells. (A) Mino cells pretreated with vehicle or ibrutinib (10, 100, or 1000 nM) were cultured alone (with anti-IgM stimulation) or in coculture with murine M2-10B4 stromal cells. M2-10B4 cells alone were pretreated with either vehicle or 100 nM ibrutinib (M2 only). Mino cells in coculture, Mino cells alone, or M2-10B4 cells alone were collected after 48 hours, lysed, and subjected to sodium dodecyl sulfate polyacrylamide gel electrophoresis and western blot analysis of pY223 BTK, pY1217 PLCγ2, pT202/Y204 ERK, pS473 AKT, and pT183/Y185 JNK. The phosphoblot was scanned, and signals were quantified (right panel); pBTK, pPLCγ2, pERK, pAKT, and pJNK signals were normalized to BTK, PLCγ2, ERK, AKT, and JNK total protein, respectively. Signals from each treatment were compared with vehicle-treated Mino cells. (B) Conditioned media from Mino cells only without stimulation, Mino cells stimulated with anti-IgM, or Mino cells in coculture with M2-10B4 or M2-10B4 alone were collected after 48 hours and analyzed for human cytokines and chemokines (IL-10, CCL22, CCL3, CCL4, TNF-α, CCL17, and CCL21). Note media from murine M2 cells alone do not react with human cytokines or chemokines.

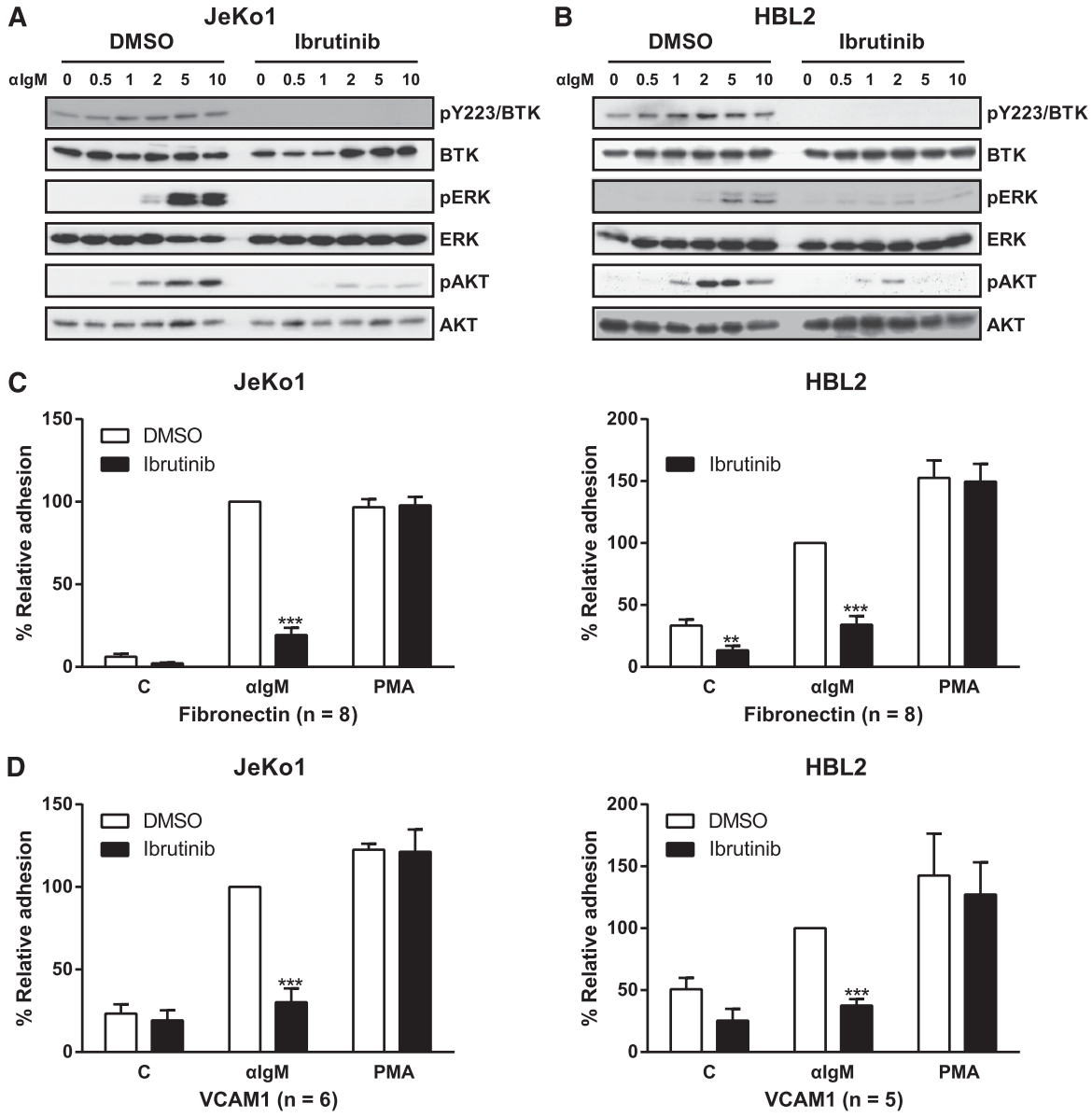

Figure 5. Ibrutinib inhibits BCR-activated adhesion of MCL cells. (A-B) Jeko1 or HBL2 cells pretreated with 100 nM ibrutinib or DMSO vehicle were stimulated with anti-IgM for 0, 0.5, 1, 2, 5, or 10 minutes and then immunoblotted for pBTK (Y223), pERK, and pAKT. (C-D) Jeko1 and HBL2 cells pretreated with drug were subjected to adhesion assays on plates precoated with anti-IgM and either (C) fibronectin or (D) VCAM-1. PMA stimulations were used as a positive control for the assay and to show specificity of drug response. The n values represent the number of independent experiments performed in triplicate; the average of these experiments is displayed. $^{**}P < .01$; $^{***}P < .001$. One-way ANOVA compared with vehicle control. PMA, phorbal 12-myristate 13-acetate.

to be in a resting stage in the circulation but may be activated in proliferation centers of tissues and LNs.[45-47] MCL cells[6,9] may also exhibit properties similar to CLL cells which, after exiting the LNs, are poised for apoptosis and/or systemic clearance. In CLL, CD38–CD31 interactions are part of a network of accessory signals that modify the microenvironment leading to the proliferation and migration of CLL cells.[48-50] CD38 expression in MCL, unlike in CLL, has not been associated with disease prognosis; however, CD38 is associated with BCR signaling and lymphocyte activation and proliferation since B lymphocytes from *xid* mice do not respond to anti-IgM or anti-CD38 while cells from wild-type mice do.[51] Recent reports indicate that positive CD38 expression in $CD23^{-}CD20^{+}$ cells with platelet counts predict the presence of t(11;14) translocation of MCL.[52] In addition, bortezomib-resistant MCL cells have higher CD38 expression.[1] To understand the precise fate of MCL cells after their exit from the tissues and LNs will require radiolabeling of patient cells such as that performed by heavy-water labeling of CLL cells and the subsequent calculation of the birth and death rate of CLL cells.[37]

We further probed the mechanisms of the increase in MCL cells by measuring cellular trafficking and PB immunophenotyping in a series of studies of cells treated with ibrutinib in vitro. We demonstrated the inhibition of BTK activity following BCR and chemokine stimulation on MCL cells alone and in coculture. Under these conditions, the drug inhibited BTK and PLCγ2 activities and reduced pERK, pJNK, and pAKT similar to the results with primary CLL cells.[7] In addition, the secretion of CCL3, CCL4, CCL22, and IL-10 was substantially reduced in Mino cell cultures and the plasma of

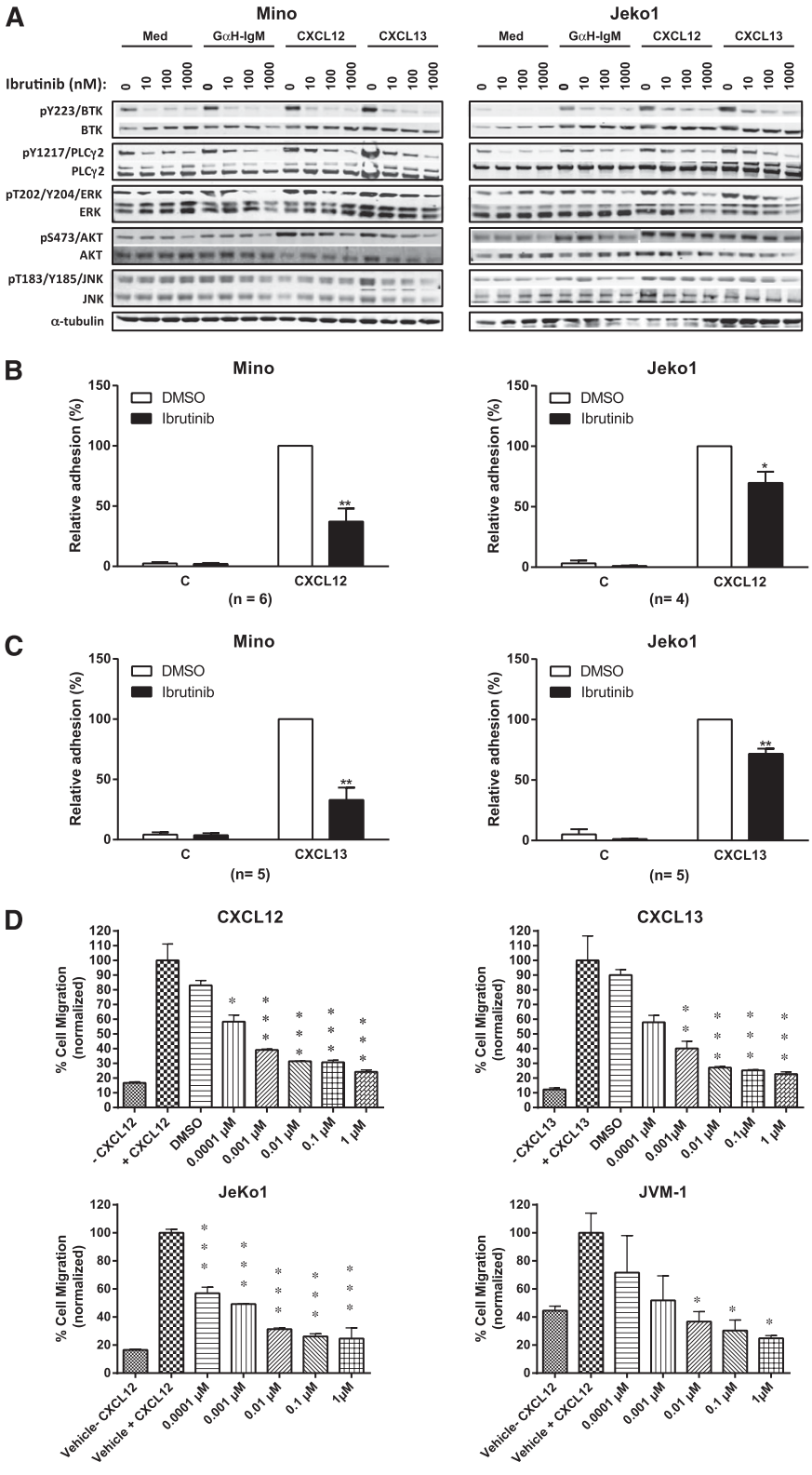

Figure 6. Ibrutinib inhibits CXCL12-/CXCL13-activated adhesion and migration of MCL cells. (A) Mino (left panel) or Jeko1 (right panel) cells pretreated with vehicle or ibrutinib 10, 100, or 1000 nM were either stimulated with anti-IgM, CXCL12, or CXCL13 or treated with medium (Med) for 15 minutes and then immunoblotted for pBTK, pPLCγ2, pAKT, pERK, and pJNK. (B-C) Mino or Jeko1 cells were treated with 100 nM ibrutinib and subjected to adhesion assays on plates precoated with (B) CXCL12 or CXCL13 and fibronectin or (C) VCAM-1. The n values represent the number of independent experiments performed in triplicate; the average of these experiments are displayed. (D) Cells from MCL cell lines Mino, Jeko1, and JVM-1 were treated with increasing concentration of ibrutinib and subjected to a chemotaxis migration assay in transwell plates with filters coated with VCAM-1, and CXCL12 or CXCL13 was added into the lower chamber as a chemoattractant. Ibrutinib dose-dependently inhibited CXCL12- and CXCL13-mediated migration of Mino cells, and CXCL12-mediated migration of Jeko1 and JVM-1 cells. $^{*}P < .05$; $^{**}P < .01$; $^{***}P < .001$. One-way ANOVA compared with vehicle control.

patients treated with ibrutinib. These results substantiate our finding on the mechanism of action of ibrutinib in MCL. Presumably, ibrutinib inhibits chemokine and BCR signaling in MCL cells in tissues and lymphoid organs, which leads to loss of adhesion and migratory ability in the microenvironment where the MCL cells are well protected and nurtured by the stromal and accessory cells. As the cells lose their adhesion to the accessory cells in the microenvironment, they exit the tissues and LNs and eventually reenter peripheral circulation. Without the microenvironment and its supply of chemokines, cytokines, and growth factors, the MCL cells cannot proliferate, and they either die within a few days and/or eventually are cleared from the circulation (Figure 7C).[53]

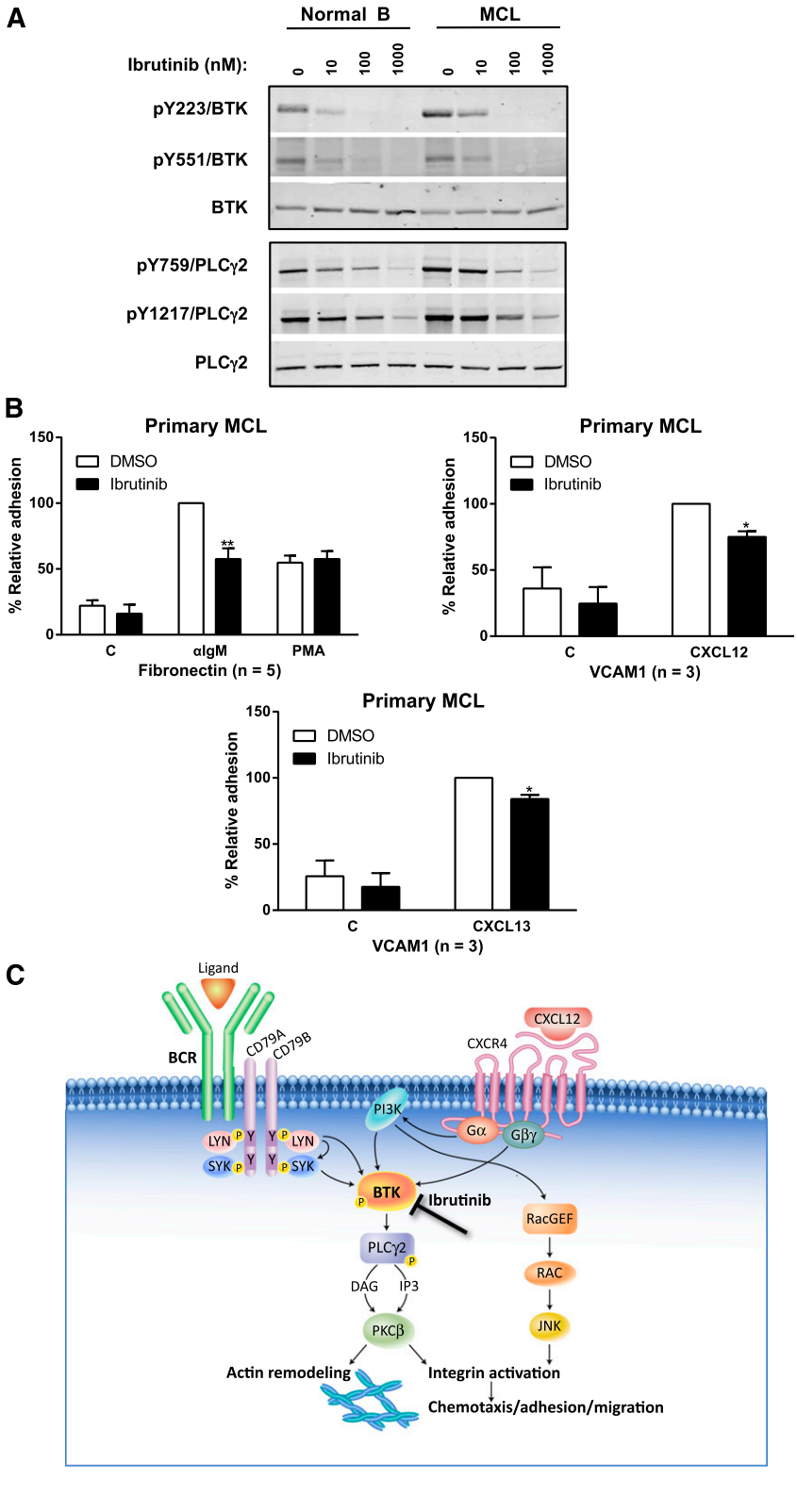

Figure 7. Ibrutinib inhibits BCR- and chemokine-induced adhesion of primary MCL cells. (A) $CD19^+$ cells isolated from PBMCs of healthy volunteers or MCL patients were treated with ibrutinib at 100 nM for 10 minutes prior to cell harvest, lysate generation, and western blotting. Primary MCL cells have increased BTK activity compared with B lymphocytes from healthy volunteers, which is further inhibited by ibrutinib in a dose-dependent manner. Tyrosine phosphorylation sites of PLC-γ are also inhibited dose-dependently by drug. (B) Ibrutinib inhibited adhesion of primary MCL cells to fibronectin- or VCAM-1–coated plates co-coated with anti-IgM, CXCL12, or CXCL13 (*$P < .05$; **$P < .01$). The n values represent the number of independent experiments performed in triplicate; the averages of these experiments are displayed. (C) Schematic of mechanism of action of ibrutinib. Since BTK is downstream to both BCR and CXCR4 signaling, ibrutinib inhibits chemokine and BCR-mediated cell adhesion/migration of malignant cells thereby disrupting the microenvironment in the tissues, LNs, and BM, which results in the malignant cells egressing and eventually entering the peripheral circulation where they are presumably cleared.

Approximately 70% of MCL patients in phase 1/2 and phase 2 clinical trials of ibrutinib have had objective clinical responses.[26,27] Our results provide important insight into the mechanism of this anti-tumor effect—inhibition of adhesion and chemokine and BCR signaling downstream of BTK—resulting in egress of malignant cells from tissues and lymphoid organs. Such effects may be inferred from the clinical observation of transiently increasing MCL cells in the PB, with concurrently decreasing lymphatic masses; here, these effects are clearly substantiated by in vitro inhibition of chemotaxis, adhesion, and migration of cells beneath stromal cells (pseudo-emperipoiesis). Moreover, we demonstrated that ibrutinib directly inhibits downstream signaling from receptors for stromal

adhesion (CXCL12 and CXCL13) as well as through BCR ligation. Once MCL cells are displaced from their microenvironment, local contact and soluble factor exposure are likely to be suboptimal for supporting cellular proliferation and survival. The cells with decreased CXCR4 expression are impaired in chemotaxis and thus fail to reenter and home into tissues. In addition, production of crucial chemokines important for homing to tissues was also apparently inhibited in vitro and in vivo. To the best of our knowledge, this is the first report that shows BTK activity to be essential for the homing of MCL cells into secondary lymphoid organs, and its inhibition results in an egress of malignant cells into PB.

Acknowledgments

The authors thank medical illustrator Jacqueline Schaffer, M.A.M.S., for editing the figures and creating Figure 7C.

This work was supported by the intramural research program of the National Heart, Lung, and Blood Institute (A.W.) and the National Cancer Institute (W.W.).

Authorship

Contribution: B.Y.C. conceived, directed, and supervised the studies, analyzed the data, and wrote the manuscript; M.F., M.F.M.D.R., P.M., S.M.S., M.M.H., A.K., S.E.M.H., and S.C. performed the experiments, analyzed the data, and contributed to the manuscript; M.S. and S.T.P. analyzed the data and contributed to the manuscript; W.W. collected samples from patients; L.E. and J.J.B. conceived the study and coordinated the collaborations between institutes; M.S., A.W., W.W., S.E.M.H., S.M.S., M.F., J.J.B., and L.E. reviewed and revised the manuscript; and all authors read and approved the final manuscript.

Conflict-of-interest disclosure: B.Y.C., M.F., P.M., M.M.H., S.C., J.J.B., and L.E. hold stock and/or stock options at Pharmacyclics, Inc. Pharmacyclics, Inc. owns patents and patent applications covering various aspects of and relating to ibrutinib. S.M.S. consults for Pharmacyclics. The remaining authors declare no competing financial interests.

Correspondence: Betty Y. Chang, Pharmacyclics, Inc., Research Department, Immunology Division, 995 E. Arques Ave, Sunnyvale, CA 94085; e-mail: bchang@pcyc.com.

References

1. Pérez-Galán P, Dreyling M, Wiestner A. Mantle cell lymphoma: biology, pathogenesis, and the molecular basis of treatment in the genomic era. *Blood.* 2011;117(1):26-38.
2. Argatoff LH, Connors JM, Klasa RJ, Horsman DE, Gascoyne RD. Mantle cell lymphoma: a clinicopathologic study of 80 cases. *Blood.* 1997;89(6):2067-2078.
3. Hoster E, Dreyling M, Klapper W, et al; German Low Grade Lymphoma Study Group (GLSG); European Mantle Cell Lymphoma Network. A new prognostic index (MIPI) for patients with advanced-stage mantle cell lymphoma. *Blood.* 2008;111(2):558-565.
4. Burger JA, Kipps TJ. Chemokine receptors and stromal cells in the homing and homeostasis of chronic lymphocytic leukemia B cells. *Leuk Lymphoma.* 2002;43(3):461-466.
5. Lenz G, Wright G, Dave SS, et al; Lymphoma/Leukemia Molecular Profiling Project. Stromal gene signatures in large-B-cell lymphomas. *N Engl J Med.* 2008;359(22):2313-2323.
6. Kurtova AV, Tamayo AT, Ford RJ, Burger JA. Mantle cell lymphoma cells express high levels of CXCR4, CXCR5, and VLA-4 (CD49d): importance for interactions with the stromal microenvironment and specific targeting. *Blood.* 2009;113(19):4604-4613.
7. de Rooij MF, Kuil A, Geest CR, et al. The clinically active BTK inhibitor PCI-32765 targets B-cell receptor- and chemokine-controlled adhesion and migration in chronic lymphocytic leukemia. *Blood.* 2012;119(11):2590-2594.
8. Medina DJ, Goodell L, Glod J, Gélinas C, Rabson AB, Strair RK. Mesenchymal stromal cells protect mantle cell lymphoma cells from spontaneous and drug-induced apoptosis through secretion of B-cell activating factor and activation of the canonical and non-canonical nuclear factor κB pathways. *Haematologica.* 2012;97(8):1255-1263.
9. Burger JA, Ford RJ. The microenvironment in mantle cell lymphoma: cellular and molecular pathways and emerging targeted therapies. *Semin Cancer Biol.* 2011;21(5):308-312.
10. Burger JA, Burger M, Kipps TJ. Chronic lymphocytic leukemia B cells express functional CXCR4 chemokine receptors that mediate spontaneous migration beneath bone marrow stromal cells. *Blood.* 1999;94(11):3658-3667.
11. Ansel KM, Ngo VN, Hyman PL, et al. A chemokine-driven positive feedback loop organizes lymphoid follicles. *Nature.* 2000;406(6793):309-314.
12. Okada T, Ngo VN, Ekland EH, et al. Chemokine requirements for B cell entry to lymph nodes and Peyer's patches. *J Exp Med.* 2002;196(1):65-75.
13. Pals ST, de Gorter DJ, Spaargaren M. Lymphoma dissemination: the other face of lymphocyte homing. *Blood.* 2007;110(9):3102-3111.
14. de Gorter DJ, Beuling EA, Kersseboom R, et al. Bruton's tyrosine kinase and phospholipase Cgamma2 mediate chemokine-controlled B cell migration and homing. *Immunity.* 2007;26(1):93-104.
15. von Andrian UH, Mempel TR. Homing and cellular traffic in lymph nodes. *Nat Rev Immunol.* 2003;3(11):867-878.
16. Burger JA. Nurture versus nature: the microenvironment in chronic lymphocytic leukemia. *Hematology Am Soc Hematol Educ Program.* 2011;2011:96-103.
17. Herishanu Y, Pérez-Galán P, Liu D, et al. The lymph node microenvironment promotes B-cell receptor signaling, NF-kappaB activation, and tumor proliferation in chronic lymphocytic leukemia. *Blood.* 2011;117(2):563-574.
18. Spaargaren M, Beuling EA, Rurup ML, et al. The B cell antigen receptor controls integrin activity through Btk and PLCgamma2. *J Exp Med.* 2003;198(10):1539-1550.
19. Stevenson FK, Krysov S, Davies AJ, Steele AJ, Packham G. B-cell receptor signaling in chronic lymphocytic leukemia. *Blood.* 2011;118(16):4313-4320.
20. Parekh S, Weniger MA, Wiestner A. New molecular targets in mantle cell lymphoma. *Semin Cancer Biol.* 2011;21(5):335-346.
21. Buggy JJ, Elias L. Bruton tyrosine kinase (BTK) and its role in B-cell malignancy. *Int Rev Immunol.* 2012;31(2):119-132.
22. Pighi C, Gu TL, Dalai I, et al. Phospho-proteomic analysis of mantle cell lymphoma cells suggests a pro-survival role of B-cell receptor signaling. *Cell Oncol (Dordr).* 2011;34(2):141-153.
23. Psyrri A, Papageorgiou S, Liakata E, et al. Phosphatidylinositol 3′-kinase catalytic subunit alpha gene amplification contributes to the pathogenesis of mantle cell lymphoma. *Clin Cancer Res.* 2009;15(18):5724-5732.
24. Rinaldi A, Kwee I, Taborelli M, et al. Genomic and expression profiling identifies the B-cell associated tyrosine kinase Syk as a possible therapeutic target in mantle cell lymphoma. *Br J Haematol.* 2006;132(3):303-316.
25. Boyd RS, Jukes-Jones R, Walewska R, Brown D, Dyer MJ, Cain K. Protein profiling of plasma membranes defines aberrant signaling pathways in mantle cell lymphoma. *Mol Cell Proteomics.* 2009;8(7):1501-1515.
26. Advani RH, Buggy JJ, Sharman JP, et al. Bruton tyrosine kinase inhibitor ibrutinib (PCI-32765) has significant activity in patients with relapsed/refractory B-cell malignancies. *J Clin Oncol.* 2013;31(1):88-94.
27. Wang L, Martin P, Blum KA, et al. The Bruton's tyrosine kinase inhibitor PCI-32765 is highly active as single-agent therapy in previously-treated mantle cell lymphoma (MCL): preliminary results of a phase II trial [abstract]. *Blood.* 2011;118(21). Abstract 442.
28. Chang BY, Huang MM, Francesco M, et al. The Bruton tyrosine kinase inhibitor PCI-32765 ameliorates autoimmune arthritis by inhibition of multiple effector cells. *Arthritis Res Ther.* 2011;13(4):R115.
29. de Gorter DJ, Reijmers RM, Beuling EA, et al. The small GTPase Ral mediates SDF-1-induced migration of B cells and multiple myeloma cells. *Blood.* 2008;111(7):3364-3372.
30. Honigberg LA, Smith AM, Sirisawad M, et al. The Bruton tyrosine kinase inhibitor PCI-32765 blocks B-cell activation and is efficacious in models of autoimmune disease and B-cell malignancy. *Proc Natl Acad Sci USA.* 2010;107(29):13075-13080.
31. Chiorazzi N. Implications of new prognostic markers in chronic lymphocytic leukemia. *Hematology Am Soc Hematol Educ Program.* 2012;2012:76-87.
32. Malavasi F, Deaglio S, Damle R, Cutrona G, Ferrarini M, Chiorazzi N. CD38 and chronic lymphocytic leukemia: a decade later. *Blood.* 2011;118(13):3470-3478.

33. Determann O, Hoster E, Ott G, et al; European Mantle Cell Lymphoma Network and the German Low Grade Lymphoma Study Group. Ki-67 predicts outcome in advanced-stage mantle cell lymphoma patients treated with anti-CD20 immunochemotherapy: results from randomized trials of the European MCL Network and the German Low Grade Lymphoma Study Group. *Blood.* 2008;111(4):2385-2387.
34. Reif K, Ekland EH, Ohl L, et al. Balanced responsiveness to chemoattractants from adjacent zones determines B-cell position. *Nature.* 2002;416(6876):94-99.
35. Allen CD, Ansel KM, Low C, et al. Germinal center dark and light zone organization is mediated by CXCR4 and CXCR5. *Nat Immunol.* 2004;5(9): 943-952.
36. Ghobrial IM, Bone ND, Stenson MJ, et al. Expression of the chemokine receptors CXCR4 and CCR7 and disease progression in B-cell chronic lymphocytic leukemia/ small lymphocytic lymphoma. *Mayo Clin Proc.* 2004;79(3):318-325.
37. Calissano C, Damle RN, Marsilio S, et al. Intraclonal complexity in chronic lymphocytic leukemia: fractions enriched in recently born/ divided and older/quiescent cells. *Mol Med.* 2011; 17(11-12):1374-1382.
38. Vlad A, Deglesne PA, Letestu R, et al. Down-regulation of CXCR4 and CD62L in chronic lymphocytic leukemia cells is triggered by B-cell receptor ligation and associated with progressive disease. *Cancer Res.* 2009;69(16):6387-6395.
39. Burger JA, Montserrat E. Coming full circle: 70 years of chronic lymphocytic leukemia cell redistribution, from glucocorticoids to inhibitors of B-cell receptor signaling. *Blood.* 2013;121(9): 1501-1509.
40. Ek S, Björck E, Högerkorp CM, Nordenskjöld M, Porwit-MacDonald A, Borrebaeck CA. Mantle cell lymphomas acquire increased expression of CCL4, CCL5 and 4-1BB-L implicated in cell survival. *Int J Cancer.* 2006;118(8):2092-2097.
41. Visser HP, Tewis M, Willemze R, Kluin-Nelemans JC. Mantle cell lymphoma proliferates upon IL-10 in the CD40 system. *Leukemia.* 2000;14(8): 1483-1489.
42. Hattori N, Nakamaki T, Ariizumi H, et al. Over-expression of CCL3 MIP-1alpha in a blastoid mantle cell lymphoma with hypercalcemia. *Eur J Haematol.* 2010;84(5):448-452.
43. Friedberg JW, Sharman J, Sweetenham J, et al. Inhibition of Syk with fostamatinib disodium has significant clinical activity in non-Hodgkin lymphoma and chronic lymphocytic leukemia. *Blood.* 2010;115(13):2578-2585.
44. Furman RR, Byrd JC, Brown JR, et al. CAL-101, an isoform-selective inhibitor of phosphatidylinositol 3-kinase p110delta, demonstrates clinical activity and pharmacodynamic effects in patients with relapsed or refractory chronic lymphocytic leukemia [abstract]. *Blood.* 2010;116:(21). Abstract 55.
45. Stein H, Bonk A, Tolksdorf G, Lennert K, Rodt H, Gerdes J. Immunohistologic analysis of the organization of normal lymphoid tissue and non-Hodgkin's lymphomas. *J Histochem Cytochem.* 1980;28(8):746-760.
46. Tsukada N, Burger JA, Zvaifler NJ, Kipps TJ. Distinctive features of "nurselike" cells that differentiate in the context of chronic lymphocytic leukemia. *Blood.* 2002;99(3):1030-1037.
47. Burger JA, Ghia P, Rosenwald A, Caligaris-Cappio F. The microenvironment in mature B-cell malignancies: a target for new treatment strategies. *Blood.* 2009;114(16):3367-3375.
48. Deaglio S, Vaisitti T, Zucchetto A, Gattei V, Malavasi F. CD38 as a molecular compass guiding topographical decisions of chronic lymphocytic leukemia cells. *Semin Cancer Biol.* 2010;20(6):416-423.
49. Deaglio S, Vaisitti T, Serra S, et al. CD38 in chronic lymphocytic leukemia: from bench to bedside? *Mini Rev Med Chem.* 2011;11(6): 503-507.
50. Deaglio S, Mallone R, Baj G, et al. CD38/CD31, a receptor/ligand system ruling adhesion and signaling in human leukocytes. *Chem Immunol.* 2000;75:99-120.
51. Lund FE, Solvason NW, Cooke MP, et al. Signaling through murine CD38 is impaired in antigen receptor-unresponsive B cells. *Eur J Immunol.* 1995;25(5):1338-1345.
52. Medd PG, Clark N, Leyden K, et al. A novel scoring system combining expression of CD23, CD20, and CD38 with platelet count predicts for the presence of the t(11;14) translocation of mantle cell lymphoma. *Cytometry B Clin Cytom.* 2011;80(4):230-237.
53. Herman SE, Gordon AL, Hertlein E, et al. Bruton tyrosine kinase represents a promising therapeutic target for treatment of chronic lymphocytic leukemia and is effectively targeted by PCI-32765. *Blood.* 2011;117(23):6287-6296.